# SPIRE Science Verification Review 2

## RAL

## September 26 2006

# Instrument Throughput

**Document Number:** SPIRE-RAL-REP-002564 iss 2

**Author(s)**
**Bruce Swinyard**
**Locke Spencer**

**Date**
**15 September 2006**

# Contents

## 1. Introduction and scope

This report details the results on the measurement of the SPIRE photometer and spectrometer passband measurements and the overall instrument transmission. These results are based on the analysis of data from PFM1; PFM2 and PFM3 test campaigns.

Between PFM2 and PFM3 the dichroics that define the band edges in the photometer were changed. Also the cryostat filter scheme was altered. Possibly affecting the measurement of the photometer bandpass.

## 2. List of requirements that the test programme was designed to evaluate

| Requirement Name | Description | Requirement |
|---|---|---|
| IRD-OPTP-R05 | Throughput | The throughput of the photometer mirrors, filters, dichroics and baffles shall be greater than 0.27 over the instrument waveband. This includes losses due to manufacturing defects; surface finish and alignment tolerances. |
| IRD-OPTP-R07 | Out of band radiation | The end to end filtering of the photometer shall control the out of band radiation to be no more than<br>$10^{-3}$ for 40 cm-1 to 200 cm-1<br>$10^{-6}$ for 200 cm-1 to 1000 cm-1<br>$10^{-9}$ for 1000 cm-1 to 100000 cm-1<br>of the in-band telescope background radiation. |
| IRD-OPTS-R05 | Theoretical throughput | The theoretical throughput of the spectrometer mirrors; filters; beam splitters and baffles shall be greater than 0.2 over the total instrument waveband including all losses due to manufacturing defects; surface finish and alignment tolerances. |
| IRD-DETP-R08 | Spectral response | ≥ 90% at the nominal edge frequencies of the appropriate passband |
| IRD-OPTS-R08 | Out of band radiation | The end-to-end filtering of the spectrometer shall control the out of band radiation to be no more than<br>$10^{-3}$ for 40 cm-1 to 200 cm-1<br>$10^{-6}$ for 200 cm-1 to 1000 cm-1<br>$10^{-9}$ for 1000 cm-1 to 100000 cm-1<br>of the in band telescope background radiation. |

## 3. Test results and conclusions

### 3.1 List of tests carried out and tests still to be done

Two basic types of test were carried out separately on the photometer and spectrometer sides of the instruments these are described in outline here.

Spectral passband measurements:

These were taken using the internal cold black body for the spectrometer – see SPIRE-RAL-REP-002566 for a report on the spectrometer bandpasses

For the photometer the spectral passband was measured using the external FTS and the hot black body source. We report on these measurements here – details of the analysis are given in the appendices.

Transmission and throughput:

The total transmission of the instrument is measured using a cold black body (CBB) that fills the instrument field of view. This can be varied in temperature and has a surface made of a polymer/crystal matrix measured to be >0.98 absorbing. By taking V-I curves with the CBB set to a series of temperatures the absorbed power onto the bolometers can be measured and compared to the expected power using a set of model assumptions for the instrument. This is discussed in section 3.3

Tests that have not been fully carried out are those concerned with testing the out of band rejection of the instrument and therefore neither IRD-OPTP-R07 or IRD-OPTS-R08 on the out of band rejection are addressed in this note although there is good evidence from the individual component measurements that this should not be a significant problem.

For a complete list of the tests carried out and the operational parameters see the test team website at http://scott1.bnsc.rl.ac.uk:8080/hcss/test_area/index.htm

### 3.2 Subsystem requirements tested at instrument level and their verification status

**IRD-DETP-R08 Detector Bandpass:** The photometer requirements as listed in the Detector Subsystem Specification Document (RD1) are:

| | | | | |
|---|---|---|---|---|
| $\lambda_b$ | **μm** | 250 | 363 | 517 |
| **Design** $\lambda_o/\Delta\lambda$ | | 3.00 | 3.18 | 3.00 |
| $\lambda_L$ **(50% points)** | **μm** | 208.3 +/- 2.1 | 306.0 +/- 3.1 | 430.8 +/- 4.3 |
| $\lambda_U$ | **μm** | 291.7 +/- 8.5 | 420.0 +/- 12.3 | 603.2 +/- 17.6 |
| $\lambda_o/\Delta\lambda$ | | 3.00 +/- 0.39 | 3.18 +/- 0.45 | 3.00 +/- 0.39 |

The differences between PFM2 and PFM3 filtering schemes is illustrated in figure 3.2-1.

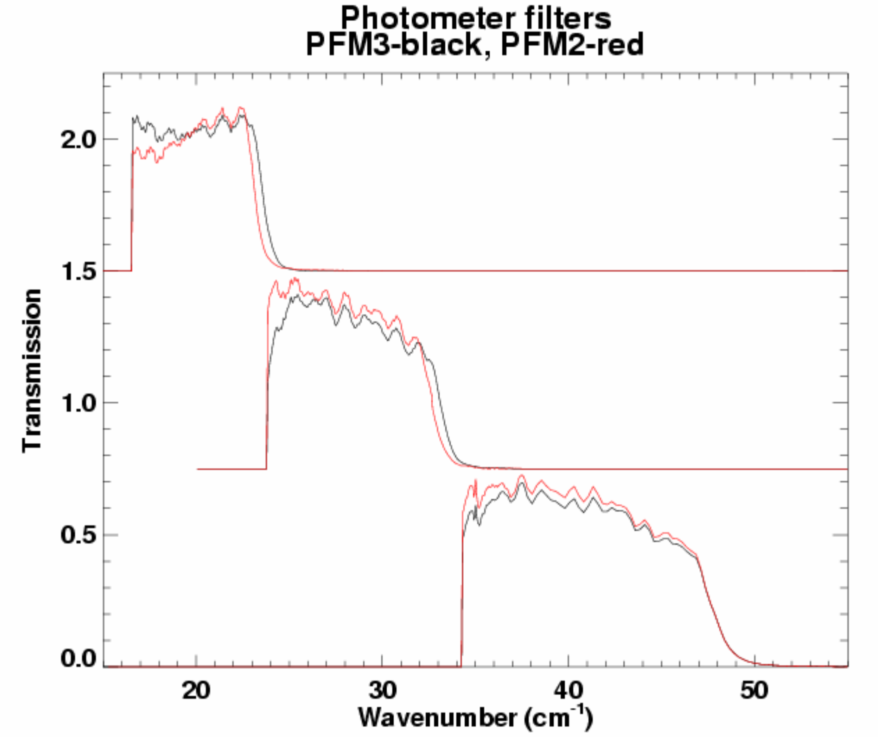


Figure 3.2-1. Laboratory measured filter profiles for the photometer in PFM2 and PFM3 test campaigns. The high frequency edges are defined by the waveguide cut offs and are shown here as brick wall filters – this is not physically correct.

The pixels measured during PFM2 and PFM3 and their measured effective band centre wavelengths and 50% band edges are given in appendices 7.1 and 7.2. Here we summarise the results concentrating on additional data from PFM3

**PLW:**

Most pixel have a short wavelength cutoff slightly lower than the requirement however they all meet the bandpass, long wavelength cutoff, and resolving power requirements. An example of a typical PLW bandpass spectrum from PFM2 is shown in figure 3.2-2 and a comparison between the expected and measured spectrum from PFM3 is shown in figure 3.2-3

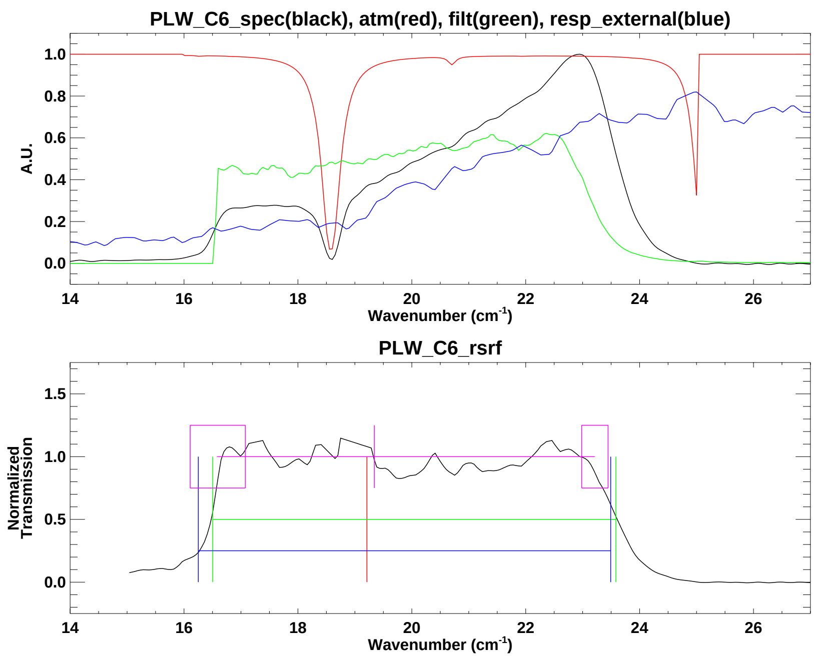


Figure 3.2-2: Spectral bandpass as measured in PFM2 for PLW shown as product of the filters and the étendue. The upper plot shows the measured spectrum (black), the atmospheric transmission (red), external calibration curve (blue), and filter calibration data (green). The lower plot shows the rsrf (black), band centre (red), bandpass and band edges at the 50% points (green). The specification bandpass and band edges with quoted tolerances are shown in pink.

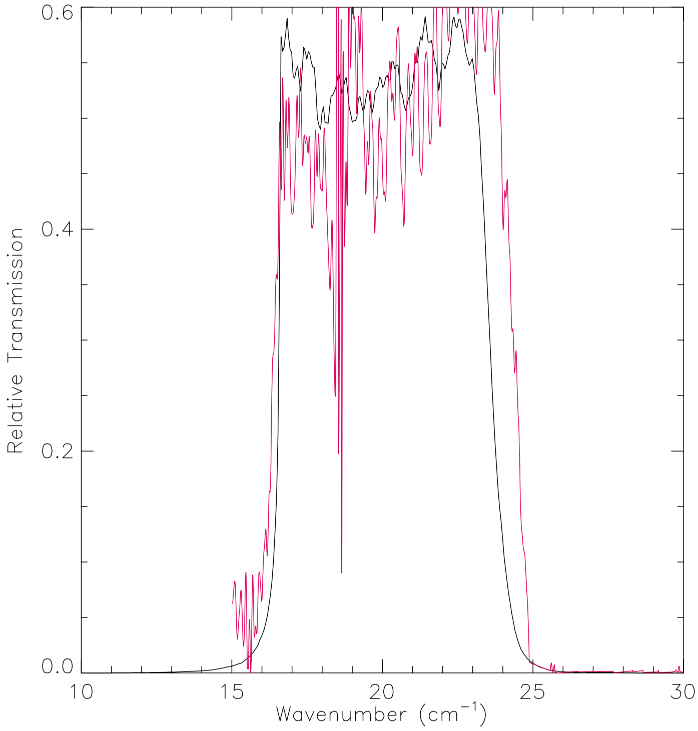


Figure 3.2-3: Spectral bandpass as measured in PFM3 for PLW C5. The laboratory measured filter transmission profile is shown black – here the waveguide cut off has been modelled with a physically realistic exponential wavelength dependence. The red curve is the net profile measured during PFM3 after removal of the black body spectrum and the atmospheric transmission. The fringing on the measured profile is thought to be due to a multiple reflection between optical components in the cryostat.

**PMW**

All of the PMW pixels measured during PFM2 have bandpasses and band edges within specification. A sample plot of the PMW bandpass spectrum from PFM2 is shown in figure 3.2-4 and a measured filter reposne from PFM3 in figure 3.2-5.

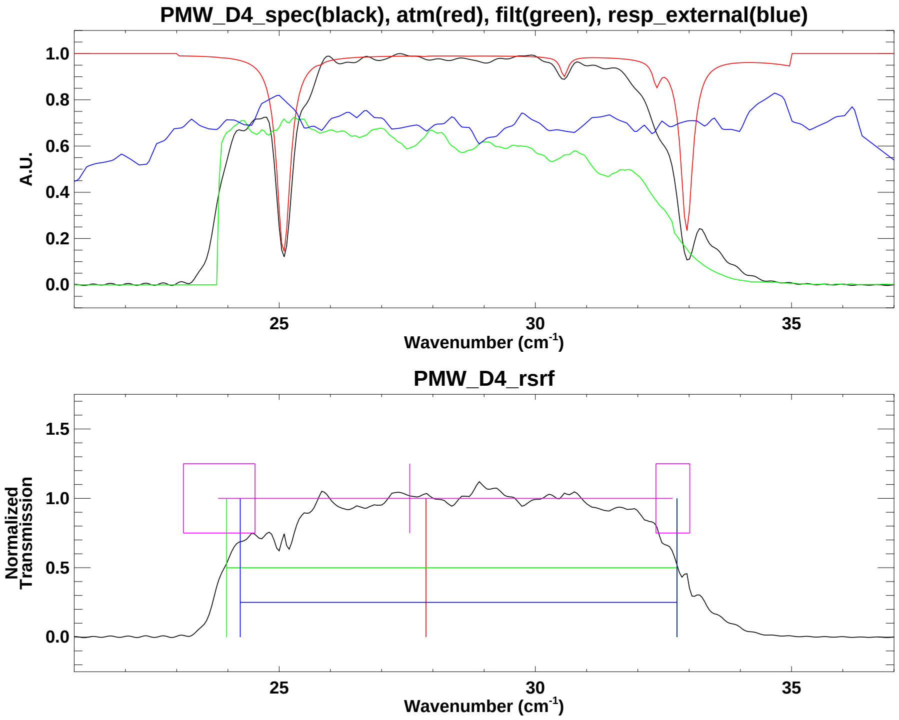


Figure 3.2-4: Spectral bandpass for PMW measured during PFM2 – see caption on figure 3.2-1 for explanation

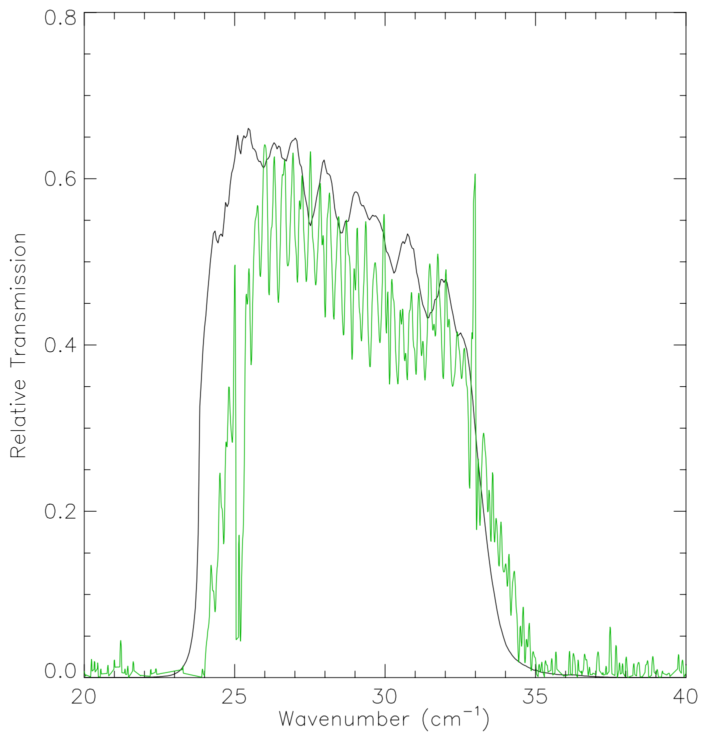


Figure 3.2-5: Spectral bandpass as measured in PFM3 for PMW D6. The laboratory measured filter transmission profile is shown black – here the waveguide cut off has been modelled with a physically realistic exponential wavelength dependence. The green curve is the net profile measured during PFM3 after removal of the black body spectrum and the atmospheric transmission. The fringing on the measured profile is thought to be due to a multiple reflection between optical components in the cryostat.

**PLW – PMW Spectral edge**

It can be seen that measured positions of the high frequency edge of PLW and the low frequency edge of PMW are significantly different to that expected from the combination of filter and waveguide spectral response – see figure 3.2-6 for a close up view. This band edge is defined by the dichroic PDIC-2 which is used in the instrument at a different angle to the measurement set up in the laboratory. We conclude therefore that, as noted in PACS for instance, that the dichroic edge has changed position and therefore PLW does not meet the specification – there is no intention to change the dichroic.

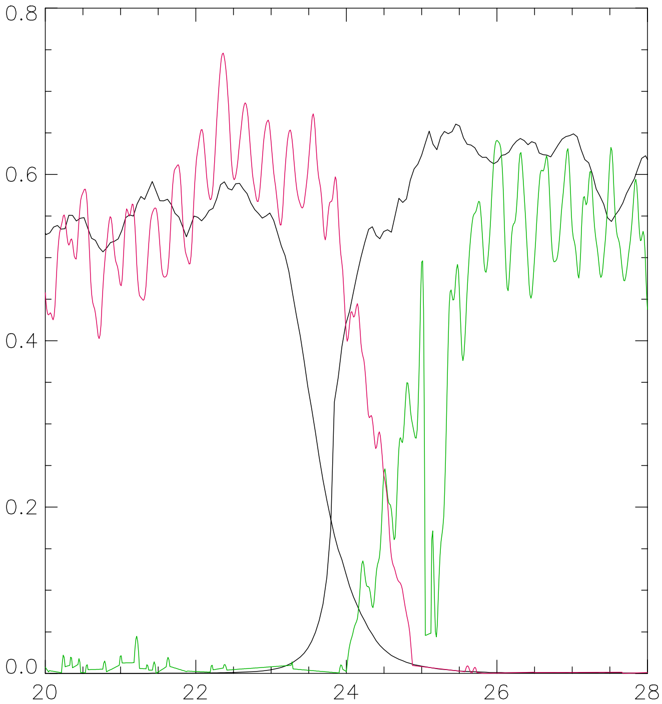


Figure 3.2-6: Close up around the spectral edge between PMW and PLW as measured in PFM3 for PLW C5 and PMW D6. The laboratory measured filter transmission profile is shown black the measurement in red and green. Not that both PLW and PMW edges have shifted to higher frequency indicating a common cause.

**PSW**

A typical PSW bandpass spectrum measured during PFM2 is shown in figure 3.2-7 and a comparison of the laboratory transmission versus wavelength and that measured during PFM3 in figure 3.2-8. It is important to note that there is significant atmospheric absorption saturation within this band and artifacts are expected in the atmospheric removal due to division by zero and imperfect fit. The data processing attempts to minimize these errors however does not completely eliminate them.

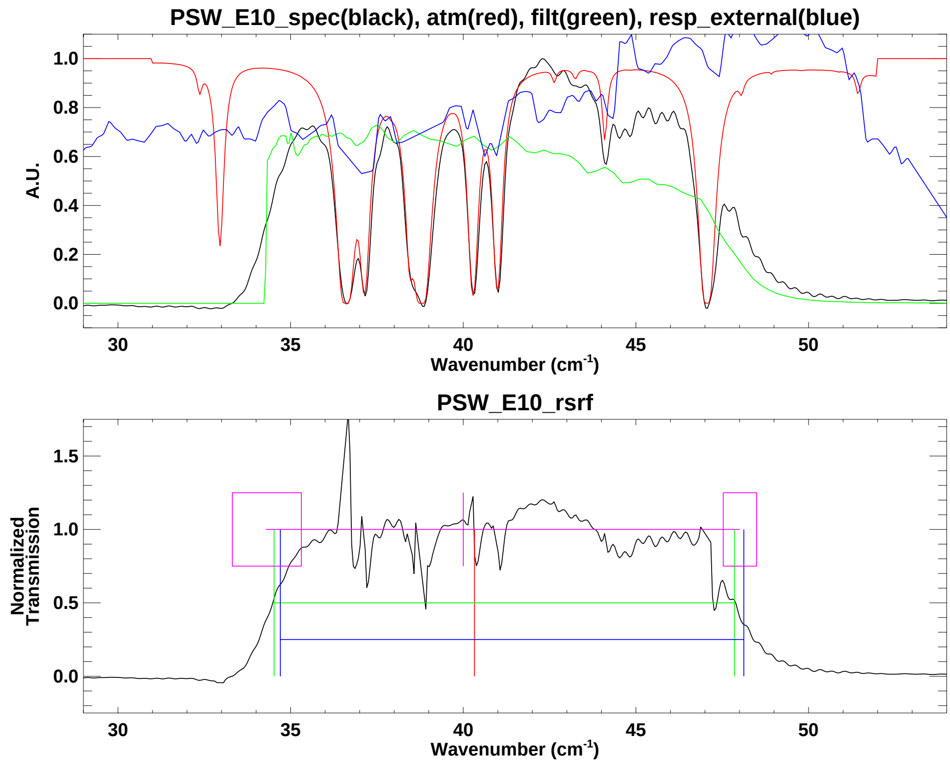


Figure 3.2-7: Spectral bandpass for PSW – see caption on figure 3.2-1 for explanation

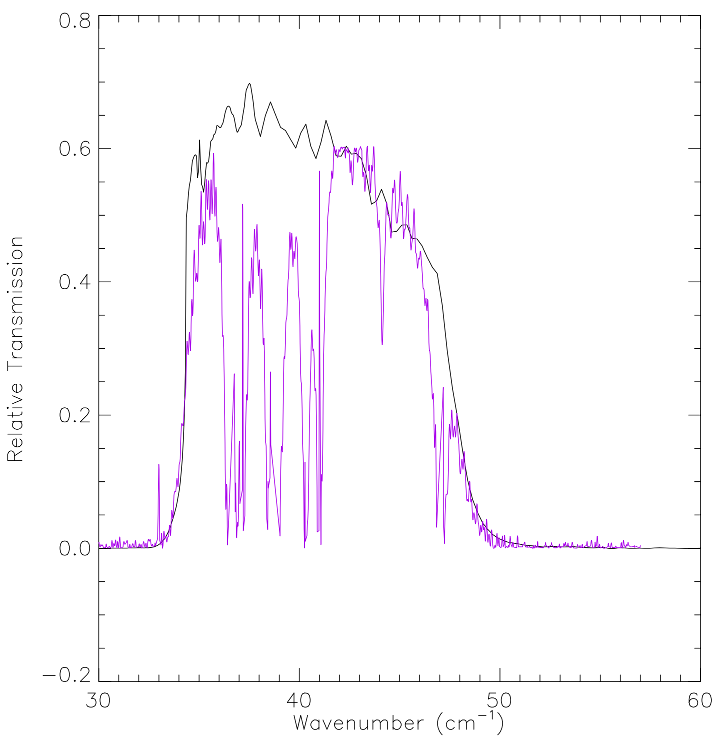


Figure 3.2-8: Spectral bandpass as measured in PFM3 for PSW E8. The laboratory measured filter transmission profile is shown black – here the waveguide cut off has been modelled with a physically realistic exponential wavelength dependence. The purple curve is the net profile measured during PFM3 after removal of the black body spectrum and a best effort to remove the atmospheric transmission which has not been as successful as usual on this high resolution spectrum. The fringing on the measured profile is thought to be due to a multiple reflection between optical components in the cryostat.

## 3.3 Instrument-level requirements and their verification status.

**IRD-OPTP-R05: Throughput**

*The throughput of the photometer mirrors, filters, dichroics and baffles shall be greater than 0.27 over the instrument waveband. This includes losses due to manufacturing defects; surface finish and alignment tolerances.*

We can test the total throughput of the system by comparing the power absorbed by the detectors to that expected taking into account our knowledge of the instrument performance as measured or estimated from measurements of the individual components and theoretical expectations – *viz.:*

| Parameter | Where derived from | Value |
|---|---|---|
| Instrument spectral bandpass | Laboratory measurements of individual filters and feedhorn specification | See figures 3.2-3,3.2-5 and 3.2-8 |
| Detector optical efficiency | Taken from the BDA EIDP | Varies |
| Etendue (AΩ) | Theoretical expected for single mode | $\lambda^2$ |
| Expected cold stop efficiency | Optical model | 0.75 |
| Loss due the hole in the BSM for PCAL | Metrology | 0.95 |
| Loss due to absorption and scattering from the mirrors | Estimate | 0.995 |
| Cold black body Emissivity | Estimate | 1.0 |

Using loadcurves taken with the CBB at 12 K and at 15 K we can measure the temperature rise and absorbed power in the detectors using the detector characteristics supplied in the EIDPs. Using the parameters in table 1 we integrate over the black body function to derive the expected absorbed power. The ratio of the measured and expected should be 1 if there are no unaccounted losses in the instrument.

As a guide the expected transmission taking an average filter transmission value and not including the feedhorn efficiency, is

0.40 – PLW
0.44 - PMW
0.48 - PSW

The test of the overall efficiency for the three arrays is presented in a graphical form in figure 3.3-1 for the case of where we compared the load with the CBB set at 12 and 15 K. We can see that there is considerable variation from pixel to pixel as confirmed by looking at the images in figure 3.3-2. Subsequent to the PFM3 test it was found that the CBB had been installed incorrectly and was misaligned compared to SPIRE causing an uneven illumination of the field of view. Despite this we can see that the maximum relative efficiency is close to 1 for all three arrays. Even with some uncertainty in the radiometric model this gives us good confidence that the throughput requirement is easily met.

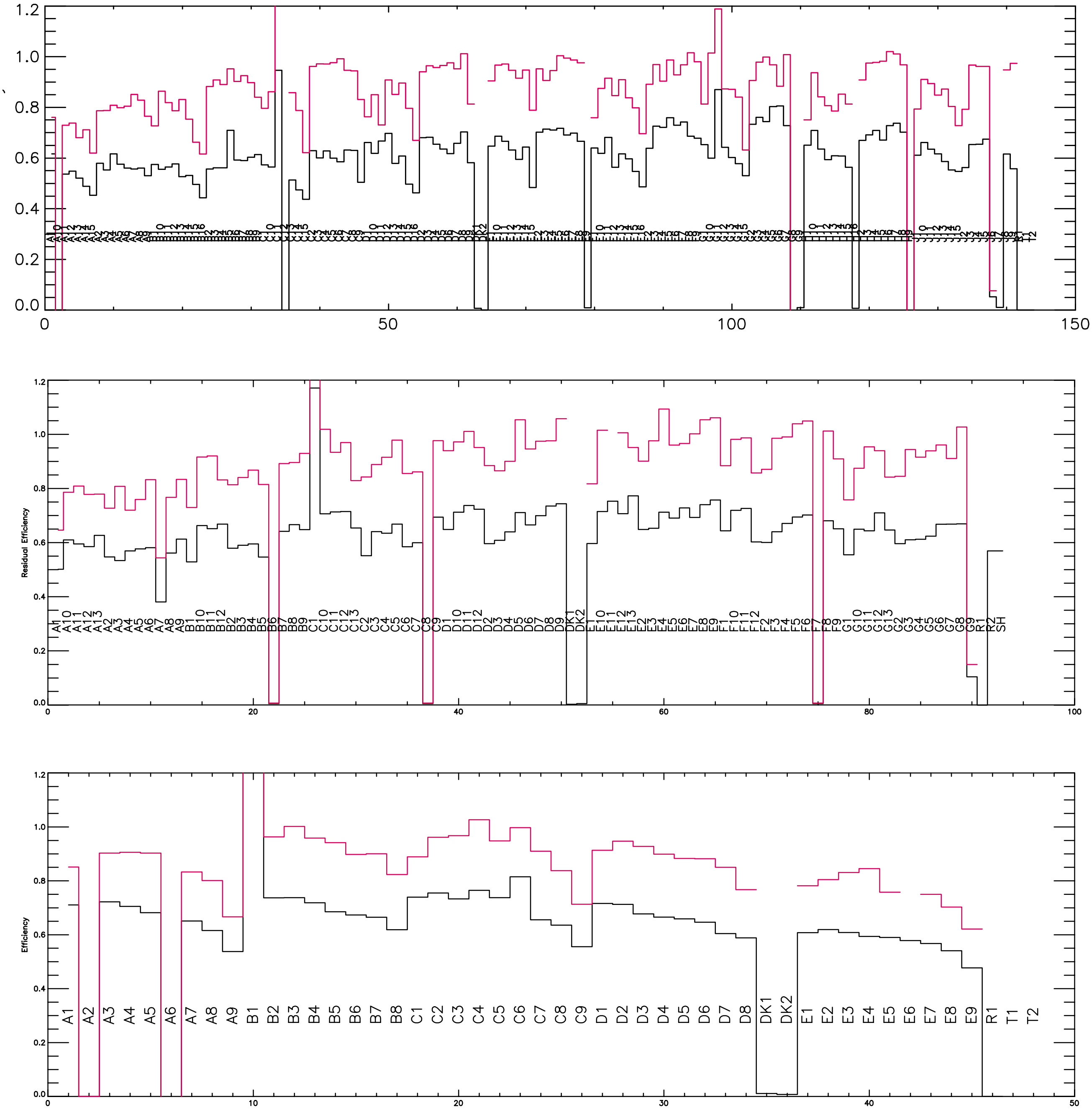


Figure 3.3-1: Ratio between measured and expected absorbed power onto the bolometers for PSW, PMW and PLW – top, middle and bottom respectively – taken from a comparison between the aborbed power with the CBB at 12 and 15 K. The black curve is before adjusting for the detector optical efficiency given by the JPL measurements and the red curve after.

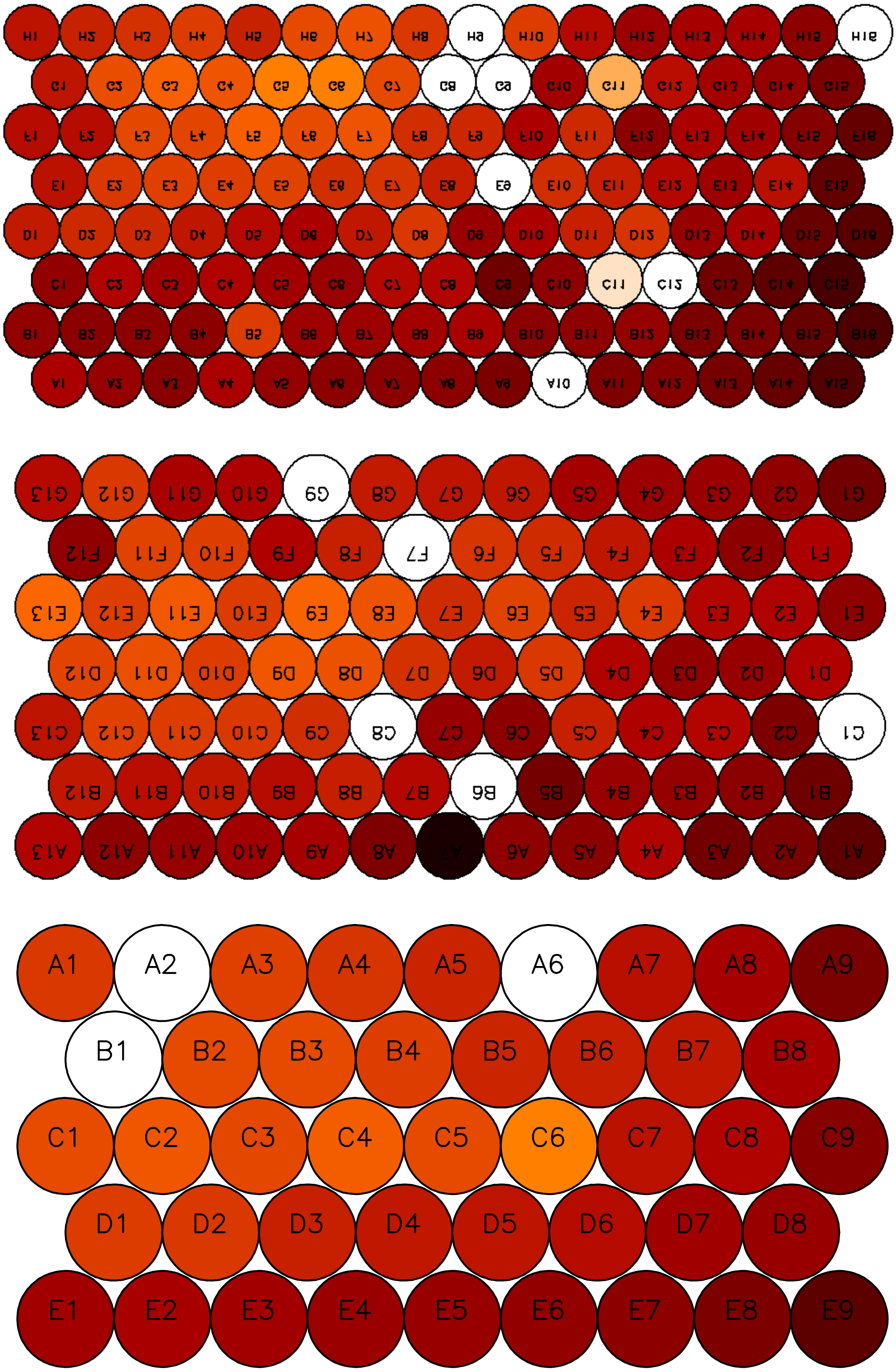


Figure 3.3-2: Image of the spatial distribution of the effective instrument transmission taken from a comparison between the aborbed power with the CBB at 12 and 15 K. The orientation of PSW and PMW are corrected to give the same "view" as PLW. The effect of the misalignment of the CBB can be clearly seen.

**IRD-OPTS-R05: Throughput**

*The theoretical throughput of the spectrometer mirrors; filters; beam splitters and baffles shall be greater than 0.2 over the total instrument waveband including all losses due to manufacturing defects; surface finish and alignment tolerances.*

The same procedure as used for the photometer was carried out on the spectrometer during PFM1 testing. The bandpass and throughput assumptions are given here. The variation of the etendue with wavelength has noew been firmly established using the beam data and associated analysis (see Optics Report RD3)

| Parameter | Where derived from | Value |
|---|---|---|
| Instrument spectral bandpass | Measurements of individual filters and feedhorn specification | See figure 3.3-3 below |
| Detector optical efficiency | Taken from the BDA EIDP | Varies |
| Etendue (AΩ) | As derived from beam measurement data | SSW – 0.12 $mm^2$ sr independent of wavelength<br>SLW - $4x10^{-6}. \lambda^2$ - $0.0045. \lambda + 1.65$ $mm^2$ sr |
| Expected cold stop efficiency | Optical model | 0.75 |
| Loss due the hole in the BSM for PCAL | Metrology | 0.95 |
| Loss due to absorption and scattering from the mirrors | Estimate | 0.99 |
| Reflectivity of the alochromed roof top mirror (2 surfaces) | Measured warm – this is a lower limit | 0.81 |
| Cold black body Emissivity | Estimate | 1.0 |

The first check made was to see if we can reconstruct the spectral variation of a black body measurement using the model parameters listed above. Figure 3.3-3 shows the model and measured spectra for the CBB at 10 K in absolute units using the radiometric model. The data for the CBB are almost always saturated (i.e. the interferogram is clipped) leading to distortions of the spectral shapes and a variation of the total in band power in the recovered spectrum. However we can see that the model is now certainly giving the correct shape and we can confidently predict the static radiometric load onto the detectors.

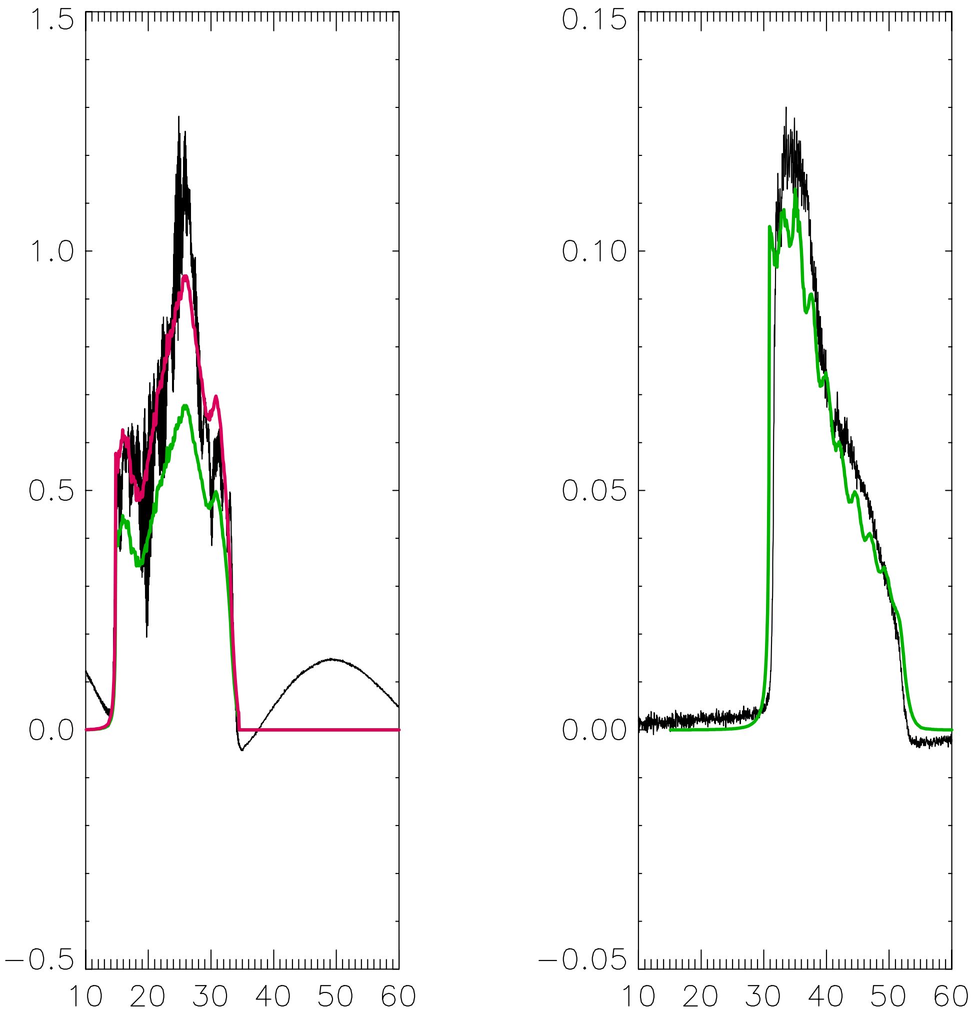


Figure3.3-3: Spectrum of the CBB at 10 K measured using the spectrometer (black curves) and as predicted from the radiometric model using the etendue established from the beam data green curve. Left is SLW and right is SSW central pixels. The red curve in the SLW plot is scaled by 1.4 to allow a better comparison of the overall shape. The units are $cm^{-1}$ in the x-axis and $W/cm^{-1}$ in the y-axis

To evaluate the transmission efficiency the CBB was set to 6.4 K and 25 K and the increase absorbed power calculated from a comparison of load curves. Figure 3.3-4 presents the derived transmission efficiencies for the two spectrometer arrays. As the efficincy appears to come out at ~0.5; a cross check was done taking the estimated power in an interferogram away from ZPD to derive the optical efficiency. This is also shown in figure 3.3-4 and we can see that this too comes out as 0.5. It is concluded that a factor of 0.5 should be introduced into the static radiometric model to account for only seeing ½ the power. We conclude therefore that the spectrometer transmission is as given by the product of the filter and expected optics losses. The etendue is rather larger than single moded and further work on the effect of this on the instrument performance is required.

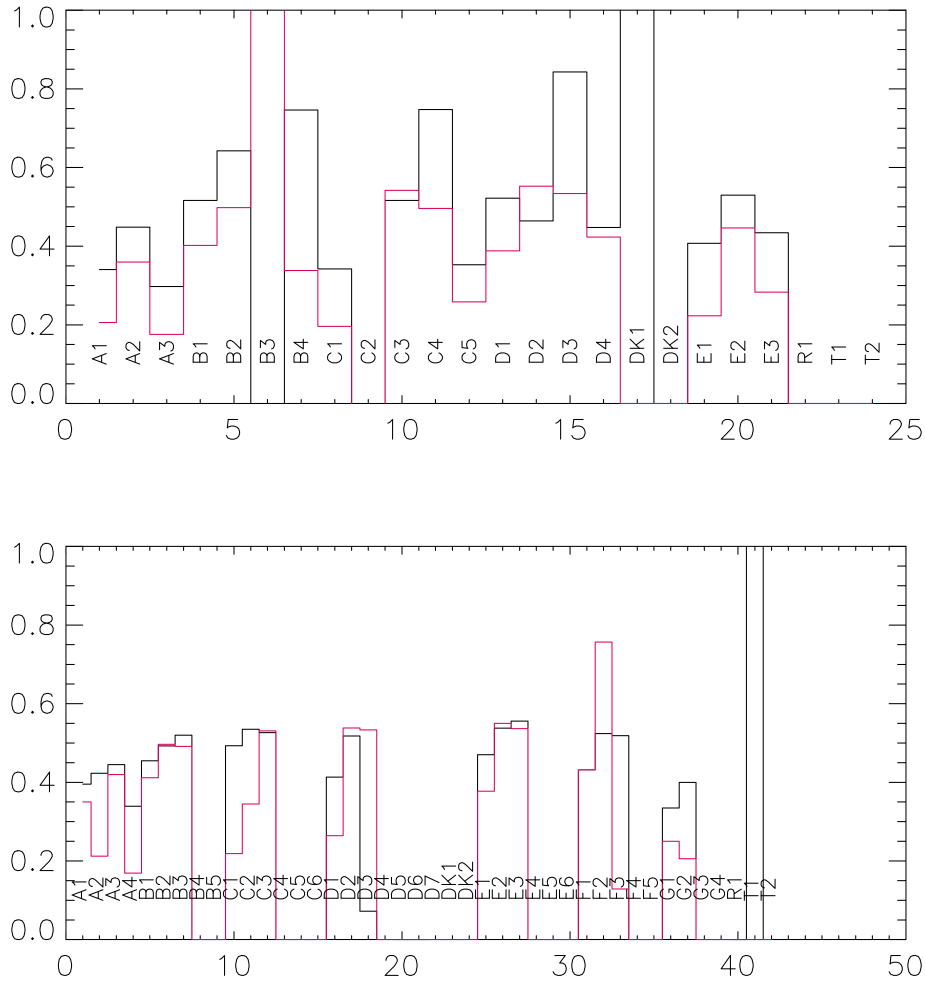


Figure 3.3-4: Ratio between measured and expected absorbed power onto the bolometers for SLW and SSW – top and bottom respectively – taken from a comparison between the absorbed power with the CBB at 6.4 and 25 K (black) and the estimated power during a spectrometer scan with the CBB at 20 K (red). The reasonable agreement between the two methods gives us confidence that there is no serious error in the calculation.

## 4. Open Issues and Anomalies

Measurements of the instrument level out of band rejection must be systematically carried out during PFM3 using the laser to check for spectral leaks.

The short wavelength PLW band edges measured do not appear to lie within the specified boundary. Many fall very close the required boundary, but not within the specified tolerance of it.

It is important to note that the external calibration curve for the TFTS and Telescope simulator was only measured using one blackbody temperature (1200C) and it is unknown whether this curve will remain accurate for other temperatures. This may effect the quality of the spectral bandpass measurements and it is recommended that the measurements are repeated at other HBB temperatures.

The spectrometer bandpass anomaly reported during SVR1 has been “resolved” however the theoretical basis for this result has not yet been fully established, nor its the full effect on the spectrometer performance.

## 5. Recommendations for further data analysis and test

**Photometer passband**

The reason for the non-compliance in the PLW/PMW passband needs to be understood.

More pixels need to be spectrally characterised in the photometer to ensure compliance over the whole array.

The cause of the fringing present in the TFTS measurements needs to be found and eliminated in order to produce high quality spectral response curves for calibration purposes.

**Spectrometer**

The spectral response to SCAL needs to be fully evaluated using the now established etendue to calibrate its spectral shape.

## References

RD1 - BDA Subsystem Specification - SPIRE-JPL-PRJ-000456
RD2 – SMEC and Spectrometer Performance - SPIRE-RAL-REP-002566
RD3 – Optical Performance Report - SPIRE-RAL-REP-002572

# 6. Appendices

## 6.1 Pixels where spectra were taken during PFM2

PLW Pixels evaluated

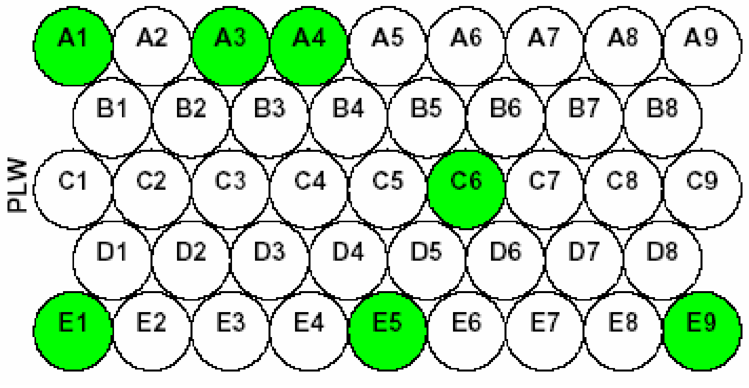


PMW Pixels evaluated


PSW Pixels evaluated

## 6.2 Measured Band Edges in PFM2

The tables in this appendix give the measured band centres and 50% band edge points for the three photometer arrays.

| specification | 517 | 172.4 +/- 18.1<br>154.3 - 190.5 | 430.8 +/- 4.3<br>426.5 - 435.1 | 603.2 +/- 17.6<br>585.6 - 620.8 | 3.00 +/- 0.39<br>2.61 - 3.39 |
|---|---|---|---|---|---|
| Pixel | $\lambda_c$ (um) | $\Delta\lambda'$ (um) | $\lambda_1'$ (um) | $\lambda_2'$ (um) | R' |
| PLW_A1 | 516.6 | 177.5 | 425.6 | 607.5 | 2.9 |
| PLW_A3 | 516.1 | 178.4 | 427.3 | 604.9 | 2.9 |
| PLW_A4 | 513.9 | 176.6 | 425.1 | 602.6 | 2.9 |
| PLW_C6 | 520.5 | 181.9 | 425.7 | 615.4 | 2.9 |
| PLW_E5 | 513.0 | 177.4 | 423.9 | 602.1 | 2.9 |
| PLW_E9 | 515.2 | 181.0 | 424.2 | 606.2 | 2.8 |

| specification | 363 | 114.0 +/- 12.7 | 306.0 +/- 3.1 | 420.0 +/- 12.3 | 3.18 +/- 0.45 |
|---|---|---|---|---|---|
| | | 101.3 - 126.7 | 302.9 - 309.1 | 407.7 - 432.3 | 2.73 - 3.63 |
| Pixel | $\lambda_c$ (um) | $\Delta\lambda'$ (um) | $\lambda_1'$ (um) | $\lambda_2'$ (um) | R' |
| PMW_A1 | 359.1 | 109.7 | 305.6 | 412.5 | 3.3 |
| PMW_A6 | 357.2 | 111.1 | 304.1 | 410.3 | 3.2 |
| PMW_A7 | 358.8 | 108.9 | 306.5 | 411.1 | 3.3 |
| PMW_B7 | 358.4 | 111.4 | 306.2 | 410.7 | 3.2 |
| PMW_C3 | 361.2 | 112.0 | 307.5 | 415.0 | 3.2 |
| PMW_C4 | 358.7 | 112.9 | 303.8 | 413.5 | 3.2 |
| PMW_C5 | 357.4 | 112.0 | 304.4 | 410.4 | 3.2 |
| PMW_C6 | 362.5 | 105.6 | 309.7 | 415.3 | 3.4 |
| PMW_D2 | 364.3 | 113.7 | 308.7 | 419.9 | 3.2 |
| PMW_D4 | 358.9 | 111.9 | 305.2 | 412.5 | 3.2 |
| PMW_F1 | 358.0 | 113.7 | 303.5 | 412.6 | 3.1 |
| PMW_G1 | 359.4 | 113.3 | 303.7 | 415.0 | 3.2 |
| PMW_G2 | 357.3 | 111.5 | 303.2 | 411.4 | 3.2 |
| PMW_G2_al | 357.8 | 111.9 | 304.1 | 411.6 | 3.2 |
| PMW_G10 | 361.8 | 114.4 | 308.0 | 415.6 | 3.2 |

| specification | 250 | 83.4 +/- 8.8 | 208.3 +/- 2.1 | 291.7 +/- 8.5 | 3.00 +/- 0.39 |
|---|---|---|---|---|---|
| | | 74.6 - 92.2 | 206.2 - 210.4 | 283.2 - 300.2 | 2.61 - 3.39 |
| Pixel | $\lambda_c$ (um) | $\Delta\lambda'$ (um) | $\lambda_1'$ (um) | $\lambda_2'$ (um) | R' |
| PSW_A8 | 247.1 | 76.6 | 209.3 | 285.0 | 3.2 |
| PSW_A9 | 247.1 | 77.8 | 209.1 | 285.2 | 3.2 |
| PSW_B8 | 247.7 | 76.0 | 209.6 | 285.9 | 3.3 |
| PSW_B9 | 249.8 | 83.0 | 209.0 | 290.5 | 3.0 |
| PSW_C10 | 248.2 | 76.3 | 210.3 | 286.0 | 3.3 |
| PSW_D10 | 247.5 | 83.6 | 206.2 | 288.7 | 3.0 |
| PSW_D11 | 251.5 | 85.5 | 210.1 | 293.0 | 2.9 |
| PSW_E9 | 249.9 | 81.9 | 208.2 | 291.5 | 3.0 |
| PSW_E10 | 248.0 | 80.7 | 207.8 | 288.2 | 3.1 |
| PSW_E12 | 248.0 | 83.0 | 207.3 | 288.8 | 3.0 |
| PSW_F12 | 248.4 | 78.9 | 210.1 | 286.7 | 3.2 |
| PSW_G12 | 249.0 | 84.2 | 208.4 | 289.7 | 3.0 |
| PSW_G13 | 249.4 | 95.3 | 209.6 | 289.3 | 2.6 |
| PSW_G13_a | 247.2 | 81.2 | 205.8 | 288.7 | 3.0 |
| PSW_G14 | 248.3 | 80.9 | 207.5 | 289.1 | 3.1 |
| PSW_H5 | 248.0 | 80.1 | 208.4 | 287.7 | 3.1 |
| PSW_H12 | 249.4 | 84.2 | 206.3 | 292.4 | 3.0 |
| PSW_H13 | 250.9 | 84.8 | 209.5 | 292.3 | 3.0 |
| PSW_H13_a | 249.9 | 84.4 | 208.7 | 291.0 | 3.0 |
| PSW_H14 | 248.7 | 83.0 | 207.4 | 289.9 | 3.0 |
| PSW_H14_a | 249.4 | 83.6 | 208.3 | 290.6 | 3.0 |
| PSW_H15 | 247.9 | 80.9 | 207.3 | 288.5 | 3.1 |
| PSW_J4 | 246.8 | 76.2 | 209.3 | 284.3 | 3.2 |
| PSW_J5 | 247.9 | 78.5 | 209.4 | 286.3 | 3.2 |
| PSW_J12 | 247.8 | 81.3 | 207.7 | 287.9 | 3.0 |
| PSW_J13 | 248.9 | 81.3 | 208.9 | 288.8 | 3.1 |
| PSW_J13_al | 248.3 | 81.1 | 208.4 | 288.2 | 3.1 |
| PSW_J14 | 248.6 | 79.7 | 209.2 | 288.0 | 3.1 |

### 6.3 Measured band edges in PFM3

**PLW**

| specification | 517 | 172.4 +/- 18.1<br>154.3 - 190.5 | 430.8 +/- 4.3<br>426.5 - 435.1 | 603.2 +/- 17.6<br>585.6 - 620.8 | 3.00 +/- 0.39<br>2.61 - 3.39 |
|---|---|---|---|---|---|
| Pixel | lc (um) | Dl (um) | l1 (um) | l2 (um) | R |
| PLW_C5 (PFM3) | 509.2 | 203.7 | 408.6 | 612.3 | 2.5 |
| PLW_C8 (PFM3) | 498.8 | 220.9 | 406.6 | 609.3 | 2.3 |

**PMW**

| | | | | | |
|---|---|---|---|---|---|
| specification | 363 | 114.0 +/- 12.7 | 306.0 +/- 3.1 | 420.0 +/- 12.3 | 3.18 +/- 0.45 |
| | | 101.3 - 126.7 | 302.9 - 309.1 | 407.7 - 432.3 | 2.73 - 3.63 |
| Pixel | lc (um) | Dl (um) | l1 (um) | l2 (um) | R |
| PMW_D4 (PFM3) | 362.3 | 108.5 | 308.1 | 416.5 | 3.2 |
| PMW_D6 (PFM3) | 356.9 | 103.6 | 305.1 | 408.8 | 3.4 |
| PMW_D7 (PFM3) | 355.7 | 112.4 | 299.5* | 411.9 | 3.3 |
| PMW_F5 (PFM3) | 361.2 | 113.1 | 304.6 | 417.7 | 3.3 |

**PSW**

| | | | | | |
|---|---|---|---|---|---|
| specification | 250 | 83.4 +/- 8.8 | 208.3 +/- 2.1 | 291.7 +/- 8.5 | 3.00 +/- 0.39 |
| | | 74.6 - 92.2 | 206.2 - 210.4 | 283.2 - 300.2 | 2.61 - 3.39 |
| Pixel | lc (um) | Dl (um) | l1 (um) | l2 (um) | R |
| PSW_C10 (PFM3) | 248.9 | 86.2 | 208.7 | 291.7 | 2.9 |
| PSW_E7 (PFM3) | 256.4 | 88.1 | 207.6 | 291.9 | 2.9 |
| PSW_E8 (PFM3) | 250.8 | 86.3 | 208.9 | 294.0 | 2.9 |